



Depósito de investigación de la Universidad de Sevilla

<https://idus.us.es/>

“This is an Accepted Manuscript of an article published by Elsevier in:
INTERNATIONAL JOURNAL OF BIOLOGICAL MACROMOLECULES
on 2021, available at: <https://doi.org/10.1016/j.ijbiomac.2021.08.043>”

1 **Rice bran-based bioplastics: effects of the mixing temperature on**
2 **starch plastification and final properties.**

3 María Alonso-González^{1,*}, Manuel Felix², Antonio Guerrero², Alberto Romero¹

4 ¹*Departamento de Ingeniería Química, Facultad de Química, Universidad de Sevilla, 41012,*
5 *Sevilla, Spain.*

6 ²*Departamento de Ingeniería Química, Escuela Politécnica Superior, Universidad de Sevilla,*
7 *41011, Sevilla, Spain.*

8

9

10

11

12

13

14

15 ***MARÍA ALONSO GONZÁLEZ**

16 *Departamento de Ingeniería Química*

17 *Universidad de Sevilla,*

18 *41011, Sevilla (Spain)*

19 *E-mail: maralonso@us.es*

20 *Phone: +34 635313411*

21 **ABSTRACT**

22 The agro-food industry produces huge amounts of wastes and by-products with high
23 levels of carbohydrates and proteins, basic food groups that, properly treated, can be
24 employed for the development of bioplastics. These high added-value products represent
25 an alternative to traditional polymers. In this research work, rice bran was mixed with
26 glycerol and water obtaining homogeneous blends which then are processed into
27 bioplastics via injection moulding. The mixing temperature aids starch plastification and
28 thus, affects the properties of the final specimens. In this way, the mechanical
29 characterization revealed improvements for the highest temperature (110 °C) used which,
30 at the same time, exhibited poor physical integrity during water immersion. Although the
31 mechanical properties of the dried system obtained at 80 °C are slightly inferior to those
32 obtained for the non-dried 110 °C system, these specimens are considered more adequate
33 since they exhibited higher physical integrity and, consequently, better operating
34 conditions.

35 **Keywords:** bioplastics; starches; injection-moulding.

36 **1. INTRODUCTION**

37 The annual production of plastics exceeded 368 million metric tons in 2019 [1]. One of
38 the main environmental impacts of plastic production is pollution, caused by its difficult
39 decomposition by microorganisms present in the soil [2]. One possible solution to solve
40 this problem is the production of eco-friendly plastics, that is, bioplastics exhibiting
41 biodegradable capacity. Bioplastics can be generated from two different sources:
42 biodegradable polyesters (petroleum-based), and biopolymers from biodegradable
43 resources [3].

44 Bioplastics formulated with plant proteins are becoming an increasingly popular source
45 of raw materials for bioplastic products, since they are not only biodegradable but are also
46 made from renewable resources, such as polysaccharides (i.e., starch), lipids and proteins
47 [4]. Bioplastics from plant proteins have been already developed based on the protein
48 content of plant protein concentrates commercially available, such as rice [5], pea [6],
49 wheat gluten [7], and soy [8] among others. In addition, a large number of studies have
50 been carried out using proteins, coming either from plant sources such as zein, wheat
51 gluten or soybean [9–11] or from animal sources such as milk proteins, collagen or gelatin
52 [12,13]. For this purpose, they are often mixed with certain plasticizers such as glycerol,
53 sorbitol, water or ethylene glycol [14], to reduce the protein-protein interactions,
54 replacing them with protein-plasticizer ones. Thus, the resulting material is suitable for
55 processing by thermomechanical techniques [15]. However, the scientific literature
56 related to the development of bioplastics based on their starch content is scarce except for
57 the research related to thermoplastic starches processed by extrusion [16,17]

58 Starch can be found in different plants, such as wheat, maize, potato and rice [18]. This
59 material has a granular structure, which consists of two main carbohydrate polymers: the
60 linear amylose and the highly branched amylopectin. Although starch is in abundance all

61 over the world, there are not many applications in material science, since the granular
62 structure must be totally destroyed in order to produce thermoplastic starch (TPS), a
63 process called gelatinization. For this purpose, starch is processed under the action of
64 temperature (between 70 and 90 °C), shearing action and water excess. Although water is
65 required, when used on its own it produces brittle products so it is often included with the
66 aid of another plasticizer [19].

67 Proteins and carbohydrates are two basic food groups that can be found in wastes from
68 the rice industry as is the case of rice bran (RB). RB is a residue from brown rice obtained
69 during the rice milling process [20]. Nowadays, this by-product is mostly used for animal
70 feeding due to its low price and nutritional richness [21]. Rice is the staple food for more
71 than half of the world's population, and yet by 2030, global rice production must double
72 to meet the demand [22] thus, emerging technologies that allow the valorization of its by-
73 products are highly convenient. The European Commission has granted projects for a
74 "near zero-waste" society such as the NoAW (No Agro-Waste) proposal [23]. In this
75 sense, the development of innovative approaches that allow the conversion of growing
76 agricultural wastes and by-products into eco-efficient bio-based products has been in the
77 spotlight in recent years. In this way, RB could be transformed into high-added-value
78 materials after suitable processing, meeting the requirements of circular economy, which
79 aims at enhancing the continuous flow of technical and biological materials while keeping
80 products, components and materials at their highest utility and value and reducing waste
81 to a minimum [24].

82 This research work aimed to analyse the effect of the mixing temperature during the
83 processing of RB-based bioplastics *via* injection moulding. The temperature employed
84 during the mixing of the raw materials is believed to be a key factor in the properties of
85 the final bioplastics specimens. In order to evaluate the effects of this parameter, different

86 mixing temperatures will be used characterizing the properties obtained by these means.
87 The different temperatures were selected with respect to the gelatinization of starch,
88 which is estimated to happen between 70 and 90 °C. In this way, the authors aim to verify
89 that temperatures around 80 °C will allow starch gelatinization, producing materials
90 suitable for injection moulding with proper mechanical and functional properties. In this
91 process, the RB/plasticizer ratio was kept constant, whereas the mixing temperature
92 varied from 50 to 110 °C. To evaluate the effects of the different mixing temperatures on
93 the final specimens, the mechanical properties were measured through frequency and
94 temperature sweep tests (rheological characterisation) and tensile tests. Finally, water
95 absorption tests were carried out to evaluate the water uptake capacity and soluble matter
96 loss, whereas SEM microscopy was employed to study the surface morphology of the
97 different specimens.

98 **2. EXPERIMENTAL**

99 **2.1 Materials**

100 The rice bran (RB) was provided by Herba Ingredients (San José de la Rinconada, Seville,
101 Spain). The by-product supplied by this company is obtained from the polishing process
102 of the rice variety “vaporized indica white rice”. This variety contains for $7.06 \pm 0.09\%$
103 moisture, $10.50 \pm 0.16\%$ ashes, $13.22 \pm 0.52\%$ proteins, $22.77 \pm 1.33\%$ lipids and
104 approximately 19 and 22 % starch and fibre, respectively (results not published yet). The
105 remaining percentage, i.e., 46.45% of the sample, can be attributed to carbohydrates,
106 according to previous works [25,26]. Water (W) and glycerol (Gly) were employed as
107 plasticizers; the former was deionized-grade water, and the latter was supplied by
108 PANREAC S.A. (Spain). All other reagents were supplied by Sigma Aldrich (USA).

109 **2.2. Processing and characterization of blends**

110 2.2.1. *Mixing of blends*

111 To obtain homogeneous blends, sieved RB (< 500 µm) along with water and glycerol
112 were introduced into a HAAKE POLYLAB QC (ThermoScientific, Germany) mixer
113 equipped with counter-rotating rotors. Water is needed in order to break the hydrogen
114 bonds present in starch, which allows its gelatinization, obtaining TPS [15]. In addition,
115 it is well established that, when used on its own, water (W) produces brittle products, thus
116 it is often used along with some other plasticizers such as glycerol (Gly) or sorbitol [27],
117 which are also compatible with proteins [8,28,29]. In this research work, different blends
118 containing 55% RB and 45% plasticizer mixture (2:1 W/Gly) were obtained by mixing
119 the raw materials for 1 h at 200 rpm, while different mixing temperatures (50, 80, 90 and
120 110 °C) were analysed to evaluate the influence of the mixing temperature used on the
121 plasticization process of RB-based bioplastics.

122 2.2.2. *Drying of blends*

123 In general, the blends mixed at 50, 80, 90 and 110 °C, which can be denoted as M50,
124 M80, M90 and M110, respectively, had to be subjected to drying to lose some of their
125 moisture content. This process was carried out in opened containers at room temperature,
126 achieving a final moisture content below 30%. Otherwise, the bioplastics obtained with
127 high moisture-containing blends exhibited voids and cracks that were easily observed,
128 probably due to the water excess that evaporated in the mould cavity, as can be seen in
129 Figure S1. It is worth mentioning that the boiling point of glycerol/water solutions is
130 strongly affected by concentration as reported in the literature [30]. Thus, the boiling point
131 of the solution containing 33,3% Gly in water is ca. 103°C, which is clearly exceeded
132 inside the mould. During this drying process, they acquired a firmer appearance, which
133 was quantified by the determination of the linear viscoelastic moduli every 24 h until they
134 were ready for injection moulding. Only the blend obtained at 110 °C was suitable for

135 injection right after the mixing stage (M110*) following the processing conditions
136 mentioned above. This is because moisture was already lower than 30% after mixing at
137 110°C. In this way, this system was the only one injected as soon as it was homogenised
138 during the mixing stage.

139 *2.2.3. Dynamic Mechanical Thermal Analysis (DMTA) of blends*

140 A dynamic mechanical analyser (RSAIII, TA Instruments, USA) was employed in
141 compression mode using a cylindrical geometry (8 mm in diameter) for each blend
142 everyday during drying. Strain sweep tests were performed at constant frequency (1 Hz)
143 and temperature to establish the linear viscoelastic region (LVR). Subsequently, the lower
144 critical strain was selected to characterize the viscoelastic modulus at 1 Hz and room
145 temperature. Finally, once the blends remained unchanged, a temperature sweep test was
146 also carried out at 5 °C/min to study the rheological behaviour of the blends between 30
147 and 160 °C. In these measurements, the storage modulus (E'), loss modulus (E'') and loss
148 tangent ($\tan \delta$) were determined for the whole temperature range studied. In addition, the
149 water content was calculated during the drying process by following the A.O.A.C.
150 methods [31]. In this way, 3 g of sample were placed in a conventional oven (Memmert
151 B216.1126, Germany) at 105 °C for 24 h to calculate the exact water content by mass
152 difference.

153 For comparison purposes, the M110 blend, was also characterized during drying to
154 evaluate this system processed under the same conditions.

155 *2.2.4. Scanning Electron Microscopy (SEM) of blends*

156 Scanning electron microscope (SEM) observations were carried out to determine the
157 importance of the mixing temperature to produce the TPS material. For this purpose, two
158 blends obtained for the same mixing velocity and time, but different mixing temperature

159 (room temperature, M20, and 80 °C, M80) were compared to another blend obtained by
160 milder conditions (M20mc, mixing for 10 min at 50 rpm and room temperature with no
161 added water) trying to observe the starch structure with minimal modifications. The
162 samples were first sputtered with a 10 nm thickness Pd/Au coating using an AC600
163 Metallizer (Leica, Germany), and then they were observed at 10 kV acceleration voltage
164 and 500x magnification.

165 **2.3 Processing and characterization of bioplastics**

166 *2.3.1. Injection moulding*

167 Each resulting blend either mixed at 50, 80, 90 or 110 °C after drying (M50, M80, M90
168 or M110) or at 110 °C right after mixing (M110*), was introduced in the cylinder of a
169 Haake pneumatic piston injection moulding equipment (MiniJet II ThermoScientific,
170 Germany) at 50 °C. The temperature of the mould was fixed at 150 °C to favour the
171 thermosetting of the specimens according to the results obtained from the temperature
172 sweep tests of the blends and a previous study [32]. Regarding injection and holding
173 pressures, they both were fixed at 500 bar, selecting 15 and 200 s for injection and holding
174 time, respectively. By employing these conditions, 60 x 10 x 1 mm rectangular bioplastic
175 specimens, denoted as I50, I80, I90, I110 and I110*, were obtained for subsequent
176 characterization.

177 *2.3.2. Dynamic Mechanical Thermal Analysis (DMTA) of bioplastics*

178 DMTA tests were carried out with an RSA-III (TA Instruments, USA) on I50, I80, I90,
179 I110 and I110* rectangular specimens using two grips, one at the bottom and one at the
180 top, to study their rheological behaviour in tension mode. Firstly, strain sweep tests were
181 performed to establish the LVR at 1 Hz and room temperature. Then, frequency sweep
182 tests were carried out within the LVR at room temperature from 0.01 to 20 Hz. Finally,

183 temperature sweep tests were also carried out within the LVR at 1 Hz between 30 and
184 140 °C using a heating rate of 5 °C/min.

185 2.3.3. Tensile tests of bioplastics

186 Tensile tests were performed with the RSA III (TA Instruments, USA) equipment in
187 continuous deformation mode. Measurements were carried out according to the ISO 527-
188 2:2012 [33], using I50, I80, I90, I110 and I110* rectangular specimens and an extensional
189 rate of 1 mm/min at room temperature. Strain-stress curves were obtained for each sample
190 and three parameters were calculated: maximum tensile strength (σ_{\max}), Young's modulus
191 (E) and strain at break (ϵ_{\max}).

192 2.3.4. Water uptake capacity of bioplastics and soluble matter loss

193 The absorption capacity of the bioplastic samples was evaluated by water uptake capacity
194 measurements following the ASTM D570 standard [34]. I50, I80, I90, I110 and I110*
195 rectangular specimens (20 x 10 x 1 mm) were used. According to the standard, the
196 samples were subjected to a dehydrothermal treatment in an oven at 50 °C for 24 h to
197 determine the initial dry weight, followed by the weighing of the sample after immersion
198 in distilled water for 24 h. Finally, the specimens were subjected to freeze-drying in a
199 LyoQuest freeze-dryer with a Flask M8 head (Telstar, Spain). Water uptake capacity
200 (WUC) and soluble matter loss (SML) were determinate by Eqs. (1) and (2):

$$201 \quad WUC (\%) = \frac{w_2 - w_3}{w_3} \cdot 100 \quad (1)$$

$$202 \quad SML (\%) = \frac{w_1 - w_3}{w_1} \cdot 100 \quad (2)$$

203 Were w_1 , w_2 and w_3 are the weights of the sample after the dehydrothermal treatment,
204 after the immersion step and after the freeze-drying stage, respectively. Samples obtained

205 after freeze-drying were denoted as F50, F80, F90, F110 and F110*, depending on the
206 initial mixing and drying conditions of the blends used.

207 *2.3.5. Scanning Electron Microscopy (SEM) of freeze-dried bioplastic matrices*

208 The microstructure of each final bioplastic after the freeze-drying treatment (F50, F80,
209 F90, F110 or F110*) was observed to determine the influence of the mixing temperature
210 on the structure generated in the bioplastics after water absorption according to the
211 protocol described by Julavittayanukul et al. [35]. The samples were first sputtered with
212 a 10 nm thickness Pd/Au coating using an AC600 Metallizer (Leica, Germany), and then
213 they were observed at 10 kV acceleration voltage and 500x magnification.

214 **2.4 Statistical analyses**

215 At least three replicates of each measurement were carried out. Statistical analyses were
216 performed using t-test and one-way analysis of variance (ANOVA) ($p < 0.05$) using the
217 STATGRAPHICS 18 software (Statgraphics Technologies, Inc, NJ, USA). Standard
218 deviations from some selected parameters were calculated. Significant differences are
219 indicated by different letters.

220 **3. RESULTS AND DISCUSSION**

221 **3.1. Characterization of blends**

222 *3.1.1. Dynamic Mechanical Thermal Analysis (DMTA) of blends*

223 Two parameters were monitored to evaluate the drying process of the blends obtained
224 after mixing: the elastic modulus at a constant frequency of 1 Hz (E_1') and the moisture
225 content (%). Figure 1 shows the evolution of these two parameters over time for the four
226 different blends obtained after mixing at 50, 80, 90 and 110 °C (M50, M80, M90 and
227 M110). As can be seen, the first three blends (M50, M80 and M90) underwent the same
228 evolution, with E_1' increasing with time for the first 6-7 days and then remaining

229 unchanged until the end of its monitoring after 10 days of drying. The values obtained
230 show no significant differences, with E_1' being slightly higher for the M80 and M90
231 blends. At the same time, the water content followed the same behaviour as the elastic
232 moduli for the different blends, observing a stabilization after drying for six days.
233 However, its values decreased during the firsts days, from 40 - 45% moisture right after
234 mixing to less than 30% at the end of the experiment, for all the studied systems. At this
235 point, the three blends were suitable for injection moulding. Moreover, the relationship
236 between both parameters shows that the elastic modulus increased when the moisture
237 content decreased, which reflects the plasticizer effect of the water contained in the
238 sample [36].

239 On the other hand, the M110 blend did not follow such a clear tendency. Right after
240 mixing (day 0), E_1' values were higher than the ones obtained for the other blends and,
241 contrary to the increasing tendency observed before, the values for this system remained
242 practically unchanged. Regarding water content, right after mixing, the moisture content
243 was low, near 20 %, due to the high temperature employed in this process (110 °C).
244 However, after 1 day, the M110 blend absorbed some moisture causing the observed
245 fluctuation. It is worth mentioning that, after several attempts, it was found that blends
246 were only suitable for injection moulding when the water content was below 30 %, and
247 no successful processing was achieved for higher values. Therefore, the moisture content
248 of the blends was found to be the critical parameter to be evaluated before proceeding
249 with injection moulding. Thus, as mentioned above, excess water (i.e. moisture higher
250 than 30%) seems to lead to severe water/glycerol evaporation inside the mould cavity,
251 which is maintained at 150°C, causing the formation of voids and cracks as can be seen
252 in Figure S1.

253 As can be observed in Figure 1, the only blend that can be readily injected after mixing is
254 the one mixed at 110°C, denoted as M110* to distinguish it from the dried blends. This
255 blend was also injected after 10 days of drying as the other systems for comparison
256 purposes, which also ensures that the moisture content was below 30%.

257 Once the blends were stabilized (i.e., 10 days after mixing), temperature sweep tests were
258 carried out between 30 and 160 °C using a heating rate of 5 °C/min. Figure 2 shows the
259 evolution of the elastic and viscous moduli (E' and E'' , respectively) with temperature.
260 Although all blends showed a predominantly elastic character, with the elastic modulus
261 being higher than the viscous modulus for the whole range studied, different behaviours
262 can be observed when the temperature increased. First, the M80 and M90 blends, show a
263 decrease in E' and E'' with increasing temperature up to 100-120 °C (from 2.6 and 1.5
264 MPa to 1.1 and 0.7 MPa, respectively). Then, both moduli increased again up to 2.0 and
265 1.3 MPa, tending to equilibrate at high temperature. For the whole temperature range,
266 both viscoelastic moduli obtained for the M80 blend are higher than those obtained for
267 M90. On the other hand, the M50 blend followed the same tendency for the first part of
268 the test (between 30 and 100-120 °C). However, above this temperature, the viscoelastic
269 moduli underwent an abrupt decrease accounting for the lowest measured values. Finally,
270 the blend mixed at 110 °C was characterized after drying for 10 days (M110), just like the
271 other systems, and right after mixing (M110*). Both blends followed a very similar
272 tendency. At the beginning of the experiment (between 30 and 70 °C), the viscoelastic
273 moduli were higher for the M110* than for M110 (e.g. E' was around 1.0 and 0.6 MPa,
274 respectively). Between 70 and 110 °C, both blends followed the same behaviour slightly
275 decreasing with increasing temperature (e.g. from 0.3 to 0.2 MPa). However, both
276 systems diverge above 110 °C up to the end of the experiment, being again M110* above
277 M110 for the higher temperatures used (at which E' values drops from 0.09 to 0.04 MPa,

278 respectively). As can be seen, M80 and M90 were the only blends that showed certain
279 thermosetting potential, with both moduli increasing above 110 °C up to 150°C. For this
280 reason, and based on the results obtained in previous studies by Alonso-González et al.
281 [32], 150°C was selected as the temperature of the mould for injection moulding. It can
282 be assumed that the higher temperatures used hinder the thermosetting potential of the
283 mixed blends leading to lower viscoelastic moduli for the whole studied range.

284 The thermosetting potential exhibited by the M80 and M90 samples has been previously
285 observed for pea protein-based blends prepared using a similar procedure at lower
286 temperatures [37]. On the other hand, Felix et al. [38] produced crayfish-based bioplastics
287 from protein/glycerol blends whose viscoelastic moduli upon temperature sweep tests
288 exhibited a decreasing tendency during the whole studied range, thus no thermosetting
289 potential was observed, showing a behaviour similar to that recorded for the two blends
290 mixed at 110 °C.

291 3.1.2. *Scanning Electron Microscopy (SEM) of blends*

292 The SEM images revealed that after mixing with mild conditions the M20mc blend still
293 contains some granular starch (Figure 3A). It can be observed that the addition of water
294 while mixing at 200 rpm for 1 h leads to a blend (M20) where the granular structure was
295 partly destroyed (Figure 3B). This structure disappeared completely for the M80 sample
296 (Figure 3C), indicating that the mixing temperature is a key parameter to obtain TPS. Tábi
297 et al. [39] obtained similar SEM images during TPS obtention through extrusion and
298 injection moulding.

299 **3.2. Characterization of bioplastics**

300 3.2.1. *Dynamic Mechanical Thermal Analysis (DMTA) of bioplastics*

301 The results obtained for the frequency sweep tests between 0.01 and 20 Hz at room
302 temperature are shown in Figure 4 for all the bioplastics injected using either the blends
303 mixed at different temperatures and dried for 10 days (I50, I80, I90 and I110) or with no
304 drying (I110*). The mechanical spectra obtained shows that E' was always higher than
305 E'' , which indicates that all specimens exhibit a predominantly elastic character [40]. The
306 viscoelastic moduli show a moderate frequency dependence, following a power-law
307 tendency to increase with increasing frequency. The power-law exponent ranges from
308 0.15 for I50 to 0.20 for I110*. This rheological behaviour has been previously observed
309 for protein-based bioplastics which exhibited slightly lower power-law exponents from
310 0.15 to 0.18 [41] and from 0.12 to 0.14 [42] for the soy/nanoclay based composites which
311 seems to indicate that the starch content induces stronger frequency dependence. In
312 addition, it should be highlighted that the higher viscoelastic moduli are found for the
313 bioplastics obtained from the blend injected right after mixing, with no drying process,
314 being clearly superior as this system exhibits 180 and 55 MPa for the elastic and viscous
315 moduli, respectively, which are clearly above the second highest one, which would be the
316 I90 system, with 68 and 23 MPa for these two parameters. The other four systems showed
317 lower viscoelastic moduli, especially the probe obtained from I110, with E'_1 being ca. 30
318 MPa, and the other three having higher and more similar values (ca. 46 and 60 MPa for
319 I50 and I80, respectively). This behaviour could be related to the fact that the system
320 obtained from the blend without drying, was injected with lower moisture content
321 (~22%), as a result of the higher mixing temperature and no water absorption during
322 drying. This fact involved a lower content of plasticizer which contributed a higher
323 viscoelastic response. However, the lower proportion of water in the plasticizer also led
324 to an increase in its boiling point, giving rise to a reduction in the evaporation inside of
325 the mould cavity [30]. The other systems (dried ones) were injected with similar water

326 contents (< 30%), and thus showed more similar values. However, the higher
327 temperatures used for the mixing stage led to slightly higher values, indicating the
328 convenience of increasing temperature during starch gelatinization. Regarding the I110
329 bioplastic, the water absorbed during drying did not take place in the gelatinization
330 process, only contributing to hindering the injection moulding stage, leading to poorer
331 results.

332 The systems were also subjected to temperature sweep tests between 30 and 140 °C
333 (Figure 5). In this case, all specimens, except the one obtained from the dried blend mixed
334 at 110 °C (I110), followed the same behaviour, with E' and E'' decreasing with increasing
335 temperature up to 90-100 °C and reaching, at this point, a plateau value, with the
336 viscoelastic moduli remaining almost unchanged. In addition, the elastic moduli began
337 clearly differentiated at 30°C, with the I110* system showing the best results (127 and 48
338 MPa for E' and E'' values, respectively), followed by the I80 and I90 systems, which
339 exhibited similar results, with 71 MPa for E' and 23-25 MPa for E'', for the two different
340 systems), with the 50 °C system showing the worst results (E' = 36 MPa and E'' = 10
341 MPa). Although, once the plateau value was reached, they all showed more similar values,
342 being the elastic modulus around 13 MPa and the viscous one approximately 3 MPa.
343 Finally, the specimens obtained from the dried blend I110 began with the same tendency,
344 where both moduli decrease with increasing temperature up to 90 °C, with the elastic
345 modulus decreasing from 16 MPa to 6 MPa although, at this point, E' and E'' underwent
346 a more abrupt decrease (about one order of magnitude), and then reached a steady value
347 around 120-140 °C, with E' stabilizing at around 0.7 MPa. Again, this differentiated
348 behaviour could be attributed to the fact that this system was the only one absorbing water
349 after the mixing stage. Thus, this water did not ease the production of TPS but hindered
350 the injection of the specimens resulting in higher sensitivity to temperature. Similar

351 tendencies can be observed for the same tests performed on defatted rice bran with similar
352 protein/starch composition processed by extrusion [17] and also with other protein-based
353 bioplastics [43].

354 *3.2.2. Tensile tests of bioplastics*

355 Figure 6 shows the stress-strain curves obtained from the tensile tests of all the samples
356 evaluated in this work. All systems exhibited a similar behaviour. The system not
357 submitted to drying exhibited the highest stiffness, although it only achieved the second-
358 lowest elongation at break. The rest of the curves presented much more similar tendencies
359 with varying parameters, with the I80 system showing the higher slope, followed by the
360 I90 system, and finally by the I50 and I110 specimens. Regarding toughness, although
361 the I90 specimens presented poorer stiffness than I80 samples, the former exhibited
362 greater elongations, leading to similar areas under the curve and therefore similar
363 toughness. To finish with, the two systems with similar slopes (50 and 110 °C) exhibited
364 quite different elongations, with the system processed at 50 °C being the one with the
365 greatest toughness and the I110 system being the one with the worst tensile properties.

366 Table 1 allows a more accurate evaluation of the three parameters obtained from the
367 stress-strain curves: Young's modulus (E), maximum tensile strength (σ_{\max}) and strain at
368 break (ϵ_{\max}). Beginning with the four systems obtained from the dried blends (I50, I80,
369 I90 and I110), it can be seen that all parameters improved when the mixing temperature
370 increased from 50 to 80 °C, although further increases had no beneficial effects, especially
371 for the system processed at 110 °C, which is in agreement with the previously mentioned
372 detrimental effect for the water absorption during drying. In this way, E increased from
373 10 ± 1 to 33 ± 6 MPa when the temperature of the mixing stage increased from 50 to 80
374 °C, although lower values (20 ± 1 and 10 ± 1 MPa) were obtained for the I90 and I110

375 systems, respectively. Again, σ_{\max} reached a maximum value for the I80 system, showing
376 its minimum value for I110 specimens. Finally, ϵ_{\max} also improved from I50 to I80 and
377 I90 systems, being the only parameter that displayed higher values for I90 than for I80
378 bioplastics. The dried system mixed at 110 °C (I110) still showed the lowest value for the
379 final elongation. Similar values have been found for protein [44] and starch-based [17]
380 systems obtained by similar processing techniques.

381 On the other hand, the system with the highest Young's modulus and tensile strength is
382 the only one that was not subjected to the drying process. The only property that did not
383 improve in this case was the elongation at break, reaching the poorest values ($1.0 \pm 0.1\%$).
384 The obtained results indicate that higher temperatures during mixing lead to stiffer
385 materials with lower elasticities. This last behaviour is typical of protein-based systems,
386 where E increases with the processing temperature, whereas the elongation at break does
387 not [8].

388 3.2.3. *Water uptake capacity of bioplastics and soluble matter loss*

389 Figure 7A shows the water uptake capacity values for the different bioplastics obtained.
390 The highest values are those obtained for the systems mixed at the highest temperature,
391 either with the dried (I110) or non-dried systems (I110*), achieving $234 \pm 21\%$, and 252
392 $\pm 75\%$, respectively. The other three systems (I50, I80 and I90) exhibited lower
393 absorption capacities, not showing any significant difference among them. These values
394 of water uptake capacity are between those typically obtained by hydrophilic protein-
395 based bioplastics [37,45,46] and those shown by starch-based specimens [47,48].
396 High water uptake capacities correspond to high soluble matter losses, as can be seen in
397 Figure 7B. In this way, the systems which underwent the highest losses were the two
398 obtained from the blends mixed at 110 °C, being 37 ± 7 and $37 \pm 16\%$ for the dried (I110)

399 and non-dried (I110*) systems, respectively. In addition, these two systems did not
400 maintain their integrity during water immersion, appearing fissures in the specimens,
401 which resulted in higher specific surfaces and, thus, higher water uptake capacity values.
402 The appearance of the fissured specimens can be seen in Figure S2. On the other hand,
403 the I50, I80 and I90 systems exhibited lower values, especially the last one with $25 \pm 1\%$.
404 The other two specimens (I50 and I80) obtained SML values of $31.6 \pm 0.3\%$ and $27 \pm$
405 1% , respectively. This result is also in line with the ones reported in the aforementioned
406 study [43].

407 These results reveal the importance of selecting a proper mixing temperature. When the
408 temperature was fixed to $50\text{ }^\circ\text{C}$, the gelatinization of starch is not achieved, leaving a
409 partial granular structure with poorer processability. Although the physical integrity is
410 not compromised, the inferior mechanical properties evidence this fact. However,
411 temperatures of 80 and $90\text{ }^\circ\text{C}$ allow complete gelatinization during mixing, providing a
412 material suitable for injection moulding that undergoes retrogradation and some
413 thermosetting phenomenon in the case of the protein fraction, resulting in specimens with
414 both good mechanical performance and physical integrity. Finally, the poorer physical
415 integrity provided by the higher temperature used could be because water is already lost
416 during mixing at $110\text{ }^\circ\text{C}$, leading to an early starch retrogradation even before injection,
417 being the bioplastic sample entirely formed through protein-related events. Regarding the
418 lipid and fibre fractions, no significant effects are expected during the bioplastics
419 processing since rice bran does not undergo any changes before $150\text{ }^\circ\text{C}$ in thermal analysis
420 [26]. However, certain fibre concentrations might have a reinforcing effect upon final
421 properties [49].

422 *3.2.4. Scanning Electron Microscopy (SEM) of freeze-dried bioplastic matrices*

423 Figure 8 shows the SEM micrographs of the different bioplastics obtained after the freeze-
424 drying stage. As can be seen, the observed morphologies match the results obtained
425 before, especially regarding functional properties, in such a way that greater surface
426 homogeneities can be associated with higher WUC, improving from samples F50 and
427 F80 (micrographs A and B) to samples F110 and F110* (micrographs C and D). It can be
428 assumed that this higher temperature led to fewer voids and fissures, and thus a more
429 homogeneous distribution of the active matter, which translates into higher absorption
430 capacities. The obtained micrographs are similar to those obtained by Tábi et al. [39] and
431 Ferreira et al. [50] for starch-based samples processed using water as the plasticizer.

432 **4. CONCLUSIONS**

433 The selected conditions, compatible with both proteins and starches, led to the successful
434 development of RB-based bioplastics by injection moulding. The mixing stage, the one
435 including the parameter under study, produced different blends that showed rheological
436 differences during and after drying. Those differences made one of them (the M110*
437 system) suitable for injection moulding right after mixing while the rest of them had to
438 undergo an drying stage in order to lose some water before being subjected to injection
439 moulding. It was concluded that, under the experimental conditions selected for the
440 injection moulding process, moisture of blends had to achieve a content lower than 30%
441 to obtain proper specimens. This limitation may be explained in terms of a reduction in
442 the boiling point of the Gly/W solution with increasing water that may induce excessive
443 evaporation from inside the mould cavity.

444 The mechanical characterization carried out on the bioplastic samples revealed two
445 superior specimens in terms of rheological and tensile parameters: the system processed
446 at 110 °C without drying (I110*) and the dried system mixed at 80 °C (I80). When water
447 uptake capacity was measured, the two systems mixed at the highest temperature (I110

448 and I110*) exhibited clearly improved values compared to the others, although they
449 exhibited much poorer physical integrities, which could be due to their high soluble
450 matter losses and the fact that they started to lose integral consistency upon water
451 immersion. These two differentiated behaviours could be associated with different
452 morphologies observed in the SEM micrographs, where the more homogeneous surfaces
453 correspond to the systems processed at higher temperatures (110 °C) leading to a more
454 successful injection-moulding processed and a greater distribution of the active matter.

455 This work evidences the possibility of manufacturing bioplastics from RB, as well as the
456 effect of water as a plasticizer, which, on the one hand, is required during the mixing
457 stage, and, on the other hand, determines the final mechanical and functional properties,
458 based on its content. A proper mixing temperature (i.e., 80 °C) is required to produce
459 suitable bioplastics with balanced properties. Furthermore, the measured properties seem
460 to be convenient for those applications that require materials exhibiting high water
461 absorption behaviour and still require suitable end-use mechanical properties, ensuring
462 their physical integrity. This should be the case of biodegradable water absorption
463 materials for healthcare, agriculture or horticulture applications. In addition, the study of
464 water uptake capacity in bioplastic systems is receiving increasing attention recently
465 because of their important applications in the fields of biomedical, pharmaceutical,
466 environmental and agricultural engineering.

467 **ACKNOWLEDGEMENTS**

468 The authors acknowledge the University of Seville for the VPPI-US grant (Ref.-II.5) to
469 Manuel Felix, and the financial support of the project RTI2018-097100-B-C21
470 (MCI/AEI/FEDER, UE) which supported this study. The authors also thank CITIUS for
471 granting access to and their assistance with the Microscopy service. The authors also
472 kindly thank Herba Ingredients for providing the raw material used in this study.

473 **REFERENCES**

- 474 [1] M. Garside, Global plastic production 1950-2019 | Statista, STATISTA. (2020).
475 [https://www.statista.com/statistics/282732/global-production-of-plastics-since-](https://www.statista.com/statistics/282732/global-production-of-plastics-since-1950/)
476 [1950/](https://www.statista.com/statistics/282732/global-production-of-plastics-since-1950/) (accessed January 28, 2021).
- 477 [2] Y. Yan, Y. Ren, X. Li, X. Zhang, H. Guo, Y. Han, J. Hu, A polysaccharide from
478 green tea (*Camellia sinensis* L.) protects human retinal endothelial cells against
479 hydrogen peroxide-induced oxidative injury and apoptosis, *Int. J. Biol.*
480 *Macromol.* 115 (2018) 600–607. <https://doi.org/10.1016/j.ijbiomac.2018.04.011>.
- 481 [3] L. Avérous, Biodegradable multiphase systems based on plasticized starch: A
482 review, *J. Macromol. Sci. - Polym. Rev.* (2004). [https://doi.org/10.1081/MC-](https://doi.org/10.1081/MC-200029326)
483 [200029326](https://doi.org/10.1081/MC-200029326).
- 484 [4] B.P. Mooney, The second green revolution? Production of plant-based
485 biodegradable plastics, *Biochem. J.* 418 (2009) 219–232.
486 <https://doi.org/10.1042/BJ20081769>.
- 487 [5] M. Félix, A. Lucio-Villegas, A. Romero, A. Guerrero, Development of rice
488 protein bio-based plastic materials processed by injection molding, *Ind. Crops*
489 *Prod.* 79 (2016) 152–159. <https://doi.org/10.1016/j.indcrop.2015.11.028>.
- 490 [6] V. Perez-Puyana, M. Felix, A. Romero, A. Guerrero, Effect of the injection
491 moulding processing conditions on the development of pea protein-based
492 bioplastics, *J. Appl. Polym. Sci.* 133 (2016) n/a-n/a.
493 <https://doi.org/10.1002/app.43306>.
- 494 [7] M. Jiménez-Rosado, L.S. Zarate-Ramírez, A. Romero, C. Bengoechea, P. Partal,
495 A. Guerrero, Bioplastics based on wheat gluten processed by extrusion, *J. Clean.*

- 496 Prod. (2019). <https://doi.org/10.1016/j.jclepro.2019.117994>.
- 497 [8] L. Fernández-Espada, C. Bengoechea, F. Cordobés, A. Guerrero, Protein/glycerol
498 blends and injection-molded bioplastic matrices: Soybean versus egg albumen, J.
499 Appl. Polym. Sci. 133 (2016) 43524. <https://doi.org/10.1002/app.42980>.
- 500 [9] B. Ghanbarzadeh, A.R. Oromiehie, M. Musavi, Z.E. D-Jomeh, E.R. Rad, J.
501 Milani, Effect of plasticizing sugars on rheological and thermal properties of zein
502 resins and mechanical properties of zein films, Food Res. Int. (2006).
503 <https://doi.org/10.1016/j.foodres.2006.05.011>.
- 504 [10] L.S. Zárate-Ramírez, A. Romero, I. Martínez, C. Bengoechea, P. Partal, A.
505 Guerrero, Effect of aldehydes on thermomechanical properties of gluten-based
506 bioplastics, Food Bioprod. Process. (2014).
507 <https://doi.org/10.1016/j.fbp.2013.07.007>.
- 508 [11] M. Yamada, S. Morimitsu, E. Hosono, T. Yamada, Preparation of bioplastic
509 using soy protein, Int. J. Biol. Macromol. 149 (2020) 1077–1083.
510 <https://doi.org/https://doi.org/10.1016/j.ijbiomac.2020.02.025>.
- 511 [12] B. Cuq, N. Gontard, S. Guilbert, Proteins as agricultural polymers for packaging
512 production, Cereal Chem. 75 (1998) 1–9.
513 <https://doi.org/10.1094/cchem.1998.75.1.1>.
- 514 [13] V. Perez-Puyana, M. Felix, L. Cabrera, A. Romero, A. Guerrero, Development of
515 gelatin/chitosan membranes with controlled microstructure by electrospinning,
516 Iran. Polym. J. 28 (2019) 921–931. <https://doi.org/10.1007/s13726-019-00755-x>.
- 517 [14] J.M. Aguilar, C. Bengoechea, E. Pérez, A. Guerrero, Effect of different polyols
518 as plasticizers in soy based bioplastics, Ind. Crops Prod. 153 (2020) 112522.

- 519 <https://doi.org/10.1016/j.indcrop.2020.112522>.
- 520 [15] T. Mekonnen, P. Mussone, H. Khalil, D. Bressler, Progress in bio-based plastics
521 and plasticizing modifications, *J. Mater. Chem. A*. 1 (2013) 13379–13398.
522 <https://doi.org/10.1039/c3ta12555f>.
- 523 [16] M. Vikman, M. Itävaara, K. Poutanen, Measurement of the biodegradation of
524 starch-based materials by enzymatic methods and composting, *J. Environ. Polym.*
525 *Degrad.* (1995). <https://doi.org/10.1007/BF02067790>.
- 526 [17] Y. Klanwan, T. Kunanopparat, P. Menut, S. Siritwattanayotin, Valorization of
527 industrial by-products through bioplastic production: Defatted rice bran and kraft
528 lignin utilization, *J. Polym. Eng.* 36 (2016) 529–536.
529 <https://doi.org/10.1515/polyeng-2015-0301>.
- 530 [18] R. Thakur, P. Pristijono, C.J. Scarlett, M. Bowyer, S.P. Singh, Q. V. Vuong,
531 Starch-based films: Major factors affecting their properties, *Int. J. Biol.*
532 *Macromol.* 132 (2019) 1079–1089.
533 <https://doi.org/10.1016/j.ijbiomac.2019.03.190>.
- 534 [19] R.F.T. Stepto, Understanding the processing of thermoplastic starch, in:
535 *Macromol. Symp.*, 2006. <https://doi.org/10.1002/masy.200651382>.
- 536 [20] I. Sereewatthanawut, S. Prapintip, K. Watchiraruji, M. Goto, M. Sasaki, A.
537 Shotipruk, Extraction of protein and amino acids from deoiled rice bran by
538 subcritical water hydrolysis, *Bioresour. Technol.* 99 (2008) 555–561.
539 <https://doi.org/10.1016/j.biortech.2006.12.030>.
- 540 [21] G.K. Chandi, D.S. Sogi, Functional properties of rice bran protein concentrates,
541 *J. Food Eng.* 79 (2007) 592–597. <https://doi.org/10.1016/j.jfoodeng.2006.02.018>.

- 542 [22] M.S. Turmel, B.L. Turner, J.K. Whalen, Soil fertility and the yield response to
543 the System of Rice Intensification, *Renew. Agric. Food Syst.* 26 (2011) 185–192.
544 <https://doi.org/10.1017/S174217051100007X>.
- 545 [23] L. Caudet, V. von Hammerstein-Gesmold, A new bioeconomy strategy for a
546 sustainable Europe, *Eur. Comm. Press Release.* (2018).
- 547 [24] Ellen MacArthur Foundation and McKinsey Center for Business and
548 Environment, *Growth within: a circular economy vision for a competitive*
549 *Europe*, 2015.
- 550 [25] Siswanti, R.B.K. Anandito, E. Nurhartadi, B.D. Iskandar, Effect of various heat
551 treatment on physical and chemical characteristics of red rice bran (*Oryza nivara*
552 L.) Rojolele, *IOP Conf. Ser. Mater. Sci. Eng.* 633 (2019) 012046.
553 <https://doi.org/10.1088/1757-899X/633/1/012046>.
- 554 [26] T. Kunanopparat, P. Menut, W. Srichumpoung, S. Siriwattanayotin,
555 Characterization of Defatted Rice Bran Properties for Biocomposite Production,
556 *J. Polym. Environ.* 22 (2014) 559–568. [https://doi.org/10.1007/s10924-014-0683-](https://doi.org/10.1007/s10924-014-0683-6)
557 [6](https://doi.org/10.1007/s10924-014-0683-6).
- 558 [27] P.M. Forssell, J.M. Mikkilä, G.K. Moates, R. Parker, Phase and glass transition
559 behaviour of concentrated barley starch-glycerol-water mixtures, a model for
560 thermoplastic starch, *Carbohydr. Polym.* 34 (1997) 275–282.
561 [https://doi.org/10.1016/s0144-8617\(97\)00133-1](https://doi.org/10.1016/s0144-8617(97)00133-1).
- 562 [28] A. Redl, M.H. Morel, J. Bonicel, S. Guilbert, B. Vergnes, Rheological properties
563 of gluten plasticized with glycerol: dependence on temperature, glycerol content
564 and mixing conditions, *Rheol. Acta.* 38 (1999) 311–320.
565 <https://doi.org/10.1007/s003970050183>.

- 566 [29] V.M. Hernandez-Izquierdo, J.M. Krochta, Thermoplastic processing of proteins
567 for film formation - A review, *J. Food Sci.* (2008). [https://doi.org/10.1111/j.1750-](https://doi.org/10.1111/j.1750-3841.2007.00636.x)
568 [3841.2007.00636.x](https://doi.org/10.1111/j.1750-3841.2007.00636.x).
- 569 [30] G.P. Association, *Physical properties of glycerine and its solutions*, 1963.
- 570 [31] AOAC, *Official Methods of Analysis of AOAC International*, 2005.
- 571 [32] A.R. M. Alonso-González, M. Felix, A. Guerrero, Effects of Mould Temperature
572 on Rice Bran-Based Bioplastics Obtained by Injection Moulding, 13 (2021) 398.
573 <https://doi.org/10.3390/polym13030398>.
- 574 [33] International Organization for Standardization, *ISO 527-1:2012 - Plastics --*
575 *Determination of tensile properties -- Part 1: General principles*, Geneva. (2012).
- 576 [34] D570, *ASTM D 570 – 98 – Standard Test Method for Water Absorption of*
577 *Plastics*, ASTM Stand. (1985). <https://doi.org/10.1520/D0570-98>.
- 578 [35] O. Julavittayanukul, S. Benjakul, W. Visessanguan, Effect of phosphate
579 compounds on gel-forming ability of surimi from bigeye snapper (*Priacanthus*
580 *tayenus*), *Food Hydrocoll.* (2006). <https://doi.org/10.1016/j.foodhyd.2005.12.007>.
- 581 [36] J. Irissin-Mangata, G. Bauduin, B. Boutevin, N. Gontard, New plasticizers for
582 wheat gluten films, *Eur. Polym. J.* 37 (2001) 1533–1541.
583 [https://doi.org/10.1016/s0014-3057\(01\)00039-8](https://doi.org/10.1016/s0014-3057(01)00039-8).
- 584 [37] V. Perez, M. Felix, A. Romero, A. Guerrero, Characterization of pea protein-
585 based bioplastics processed by injection moulding, *Food Bioprod. Process.* 97
586 (2016) 100–108. <https://doi.org/10.1016/j.fbp.2015.12.004>.
- 587 [38] M. Felix, A. Romero, F. Cordobes, A. Guerrero, Development of crayfish bio-
588 based plastic materials processed by small-scale injection moulding, *J. Sci. Food*

- 589 Agric. 95 (2015) 679–687. <https://doi.org/10.1002/jsfa.6747>.
- 590 [39] T. Tábi, J.G. Kovács, Examination of injection moulded thermoplastic maize
591 starch, *Express Polym. Lett.* 1 (2007) 804–809.
592 <https://doi.org/10.3144/expresspolymlett.2007.111>.
- 593 [40] H.A. Barnes, *A Handbook of Elementary Rheology*, University of Wales,
594 Institute of Non-Newtonian Fluid Mechanics, Wales, 2000.
- 595 [41] V. Bourny, V. Perez-Puyana, M. Felix, A. Romero, A. Guerrero, Evaluation of
596 the injection moulding conditions in soy/nanoclay based composites, *Eur. Polym.*
597 *J.* 95 (2017) 539–546.
598 <https://doi.org/https://doi.org/10.1016/j.eurpolymj.2017.08.036>.
- 599 [42] M. Felix, I. Martinez, A. Romero, P. Partal, A. Guerrero, Effect of pH and
600 nanoclay content on the morphology and physicochemical properties of soy
601 protein/montmorillonite nanocomposite obtained by extrusion, *Compos. Part B*
602 *Eng.* 140 (2018) 197–203.
603 <https://doi.org/https://doi.org/10.1016/j.compositesb.2017.12.040>.
- 604 [43] V. Perez, M. Felix, A. Romero, A. Guerrero, Characterization of pea protein-
605 based bioplastics processed by injection moulding, *Food Bioprod. Process.* 97
606 (2016) 100–108. <https://doi.org/10.1016/j.fbp.2015.12.004>.
- 607 [44] M. Felix, V. Perez-Puyana, A. Romero, A. Guerrero, Production and
608 Characterization of Bioplastics Obtained by Injection Moulding of Various
609 Protein Systems, *J. Polym. Environ.* 25 (2017) 91–100.
610 <https://doi.org/10.1007/s10924-016-0790-7>.
- 611 [45] L. Fernández-Espada, C. Bengoechea, F. Cordobés, A. Guerrero,

- 612 Thermomechanical properties and water uptake capacity of soy protein-based
613 bioplastics processed by injection molding, *J. Appl. Polym. Sci.* 133 (2016)
614 43524. <https://doi.org/10.1002/app.43524>.
- 615 [46] E. Álvarez-Castillo, A. Del Toro, J.M. Aguilar, A. Guerrero, C. Bengoechea,
616 Optimization of a thermal process for the production of superabsorbent materials
617 based on a soy protein isolate, *Ind. Crops Prod.* 125 (2018) 573–581.
618 <https://doi.org/10.1016/j.indcrop.2018.09.051>.
- 619 [47] J. Yang, Y.C. Ching, C.H. Chuah, N.S. Liou, Preparation and characterization of
620 starch/empty fruit bunch-based bioplastic composites reinforced with epoxidized
621 oils, *Polymers (Basel)*. 13 (2021) 1–15. <https://doi.org/10.3390/polym13010094>.
- 622 [48] S.W. Lusiana, D. Putri, I.Z. Nurazizah, Bahruddin, Bioplastic Properties of Sago-
623 PVA Starch with Glycerol and Sorbitol Plasticizers, *J. Phys. Conf. Ser.* 1351
624 (2019) 0–8. <https://doi.org/10.1088/1742-6596/1351/1/012102>.
- 625 [49] S. Gamero, M. Jiménez-Rosado, A. Romero, C. Bengoechea, A. Guerrero,
626 Reinforcement of Soy Protein-Based Bioplastics Through Addition of
627 Lignocellulose and Injection Molding Processing Conditions, *J. Polym. Environ.*
628 2019 276. 27 (2019) 1285–1293. <https://doi.org/10.1007/S10924-019-01430-1>.
- 629 [50] W.H. Ferreira, M.M.I.B. Carmo, A.L.N. Silva, C.T. Andrade, Effect of structure
630 and viscosity of the components on some properties of starch-rich hybrid blends,
631 *Carbohydr. Polym.* 117 (2015) 988–995.
632 <https://doi.org/10.1016/j.carbpol.2014.10.018>.
- 633

634 **FIGURE CAPTIONS**

635 **Figure 1:** Fit of the elastic modulus at 1 Hz (E_1') and moisture content over drying time
636 of the M50, M80, M90 and M110 blends. The injectability limit (i.e. the maximum
637 moisture content below which the blends can be injected) is also shown.

638 **Figure 2:** Temperature sweep tests at 5°C/min between 30 and 160 °C for the blends
639 obtained after mixing at different temperatures and drying for 10 days (M50, M80, M90
640 and M110) or mixed at 110 °C with no drying (M110*).

641 **Figure 3.** SEM micrographs of the blends obtained by mixing (A) at 50 rpm for 10 min,
642 room temperature and no added water (M20mc) (B) at 200 rpm for 1h and room
643 temperature (M20) and (C) at 200 rpm for 1h and 80 °C (M80).

644 **Figure 4.** Frequency sweep tests between 0.01 and 20 Hz for the bioplastics obtained
645 from the different blends after drying for 10 days (I50, I80, I90 and I110) and with no
646 drying (I110*).

647 **Figure 5.** Temperature sweep tests at 5°C/min between 30 and 140 °C for the bioplastics
648 obtained from the different blends after drying for 10 days (I50, I80, I90 and I110) and
649 with no drying (I110*).

650 **Figure 6.** Stress-strain curves from the tensile tests performed on the bioplastic samples
651 obtained from the different blends (I50, I80, I90 and I110) and with no drying (I110*).

652 **Figure 7.** (A) Water uptake capacity (WUC) and (B) soluble matter loss (SML) of the
653 bioplastic samples obtained from the different blends: mixed at 50, 80, 90 and 110 °C
654 after drying and mixed at 110 °C with no drying (110 °C*).

655 **Figure 8.** SEM micrographs of the bioplastic samples obtained after freeze-drying of
656 bioplastics processed from different blends (A) F50, (B) F80, (C) F110 and (D) F110*.

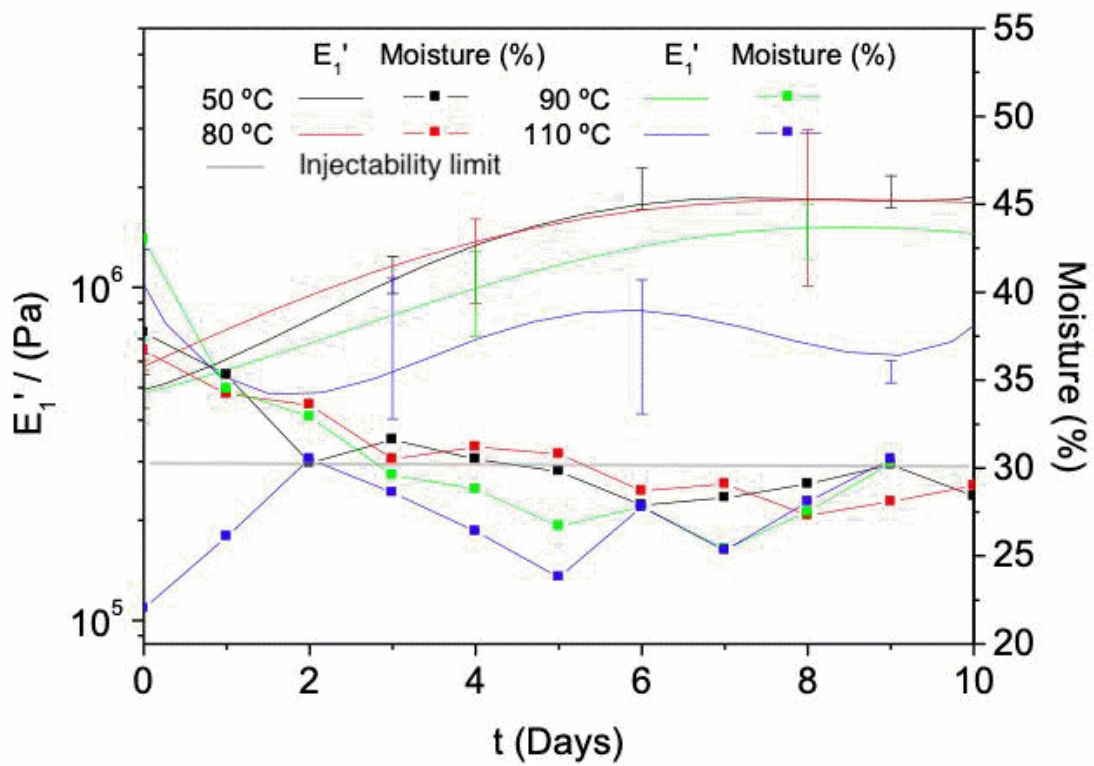


Figure 1.

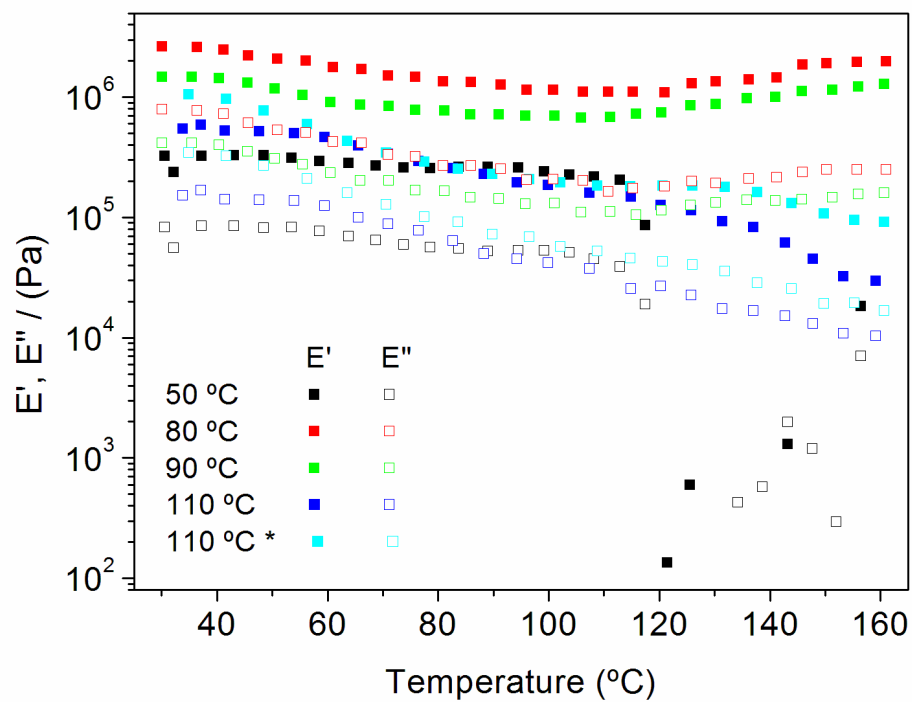


Figure 2

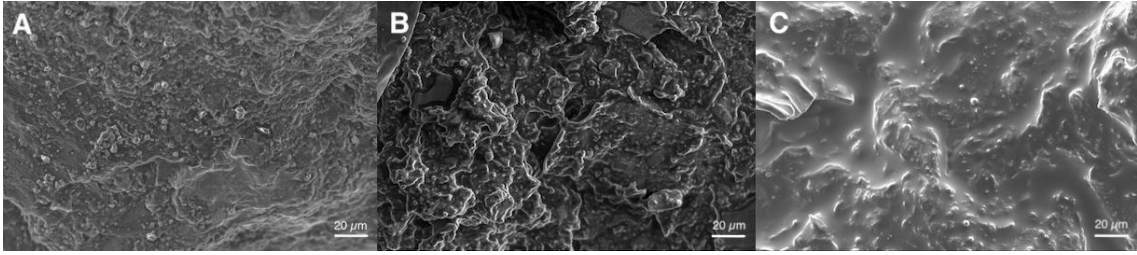


Figure 3

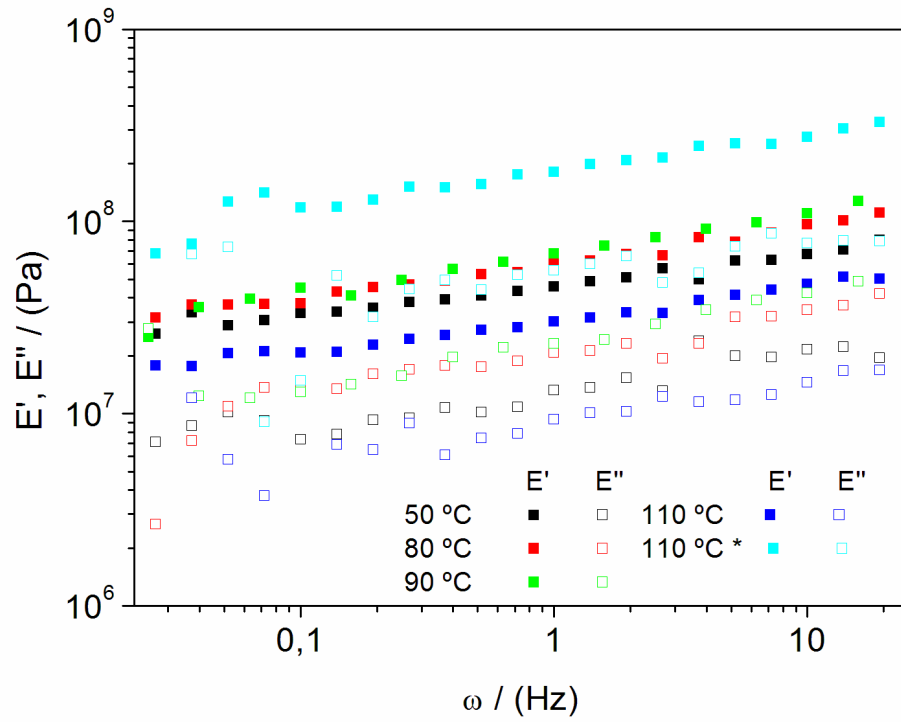


Figure 4

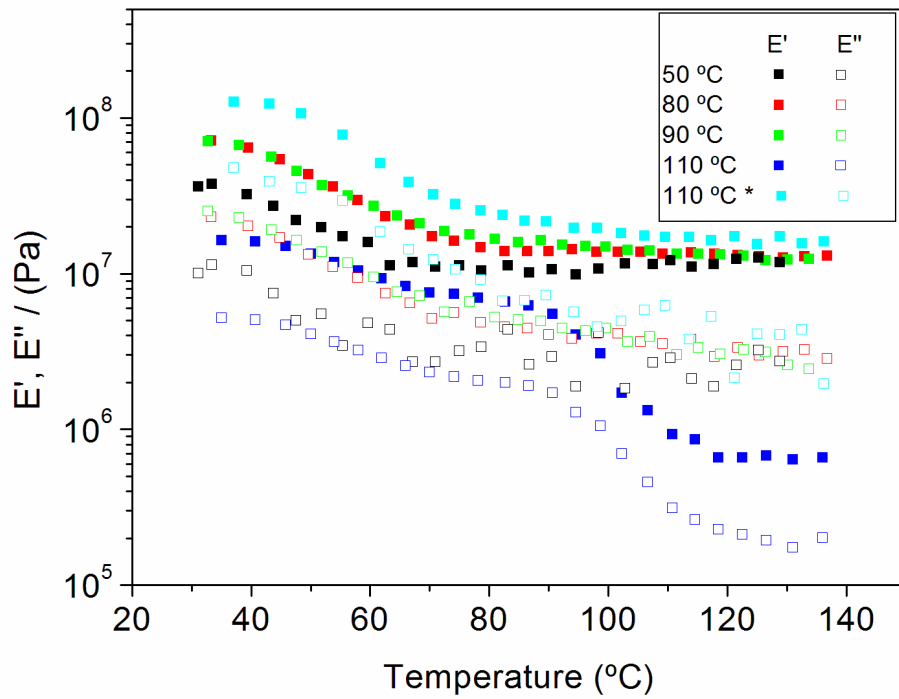


Figure 5

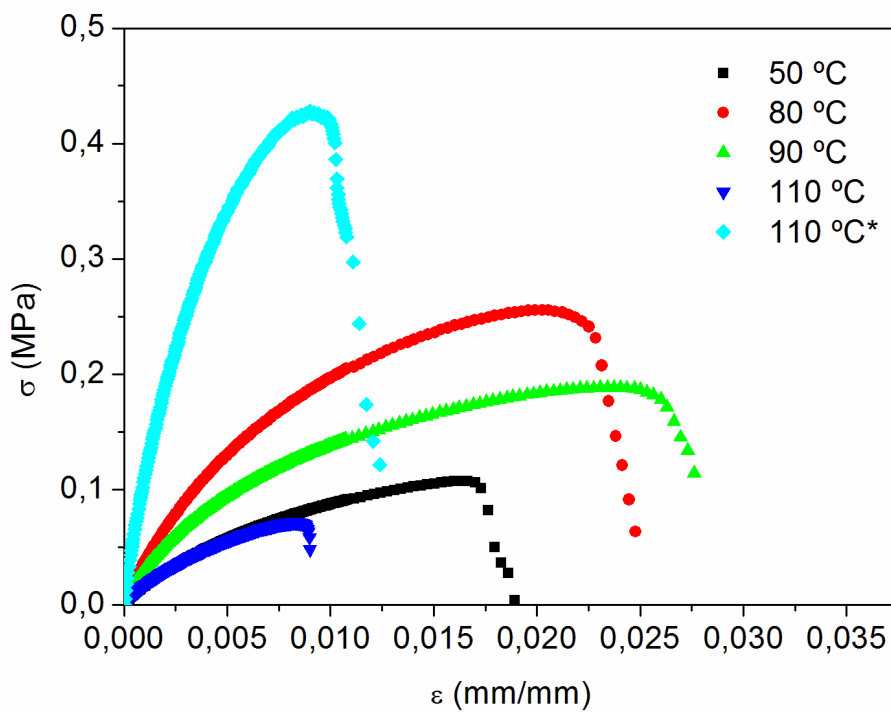


Figure 6

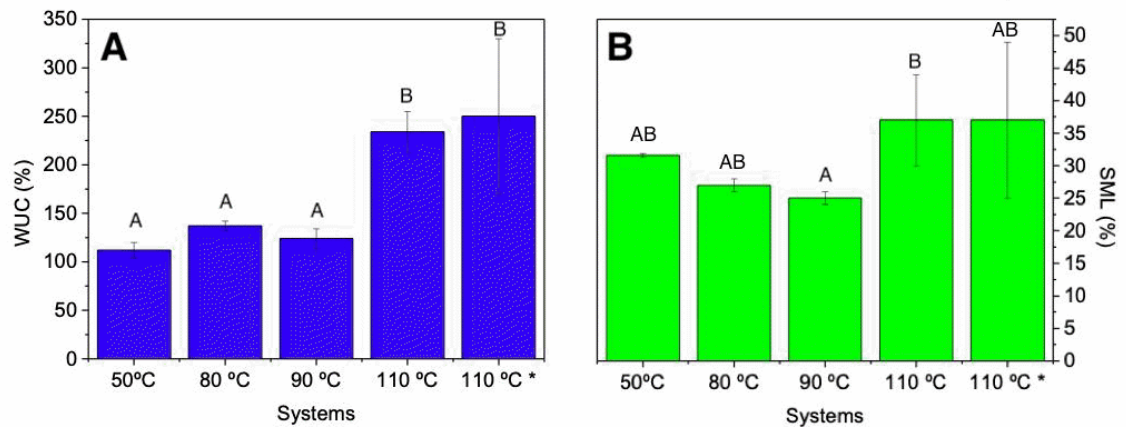


Figure 7

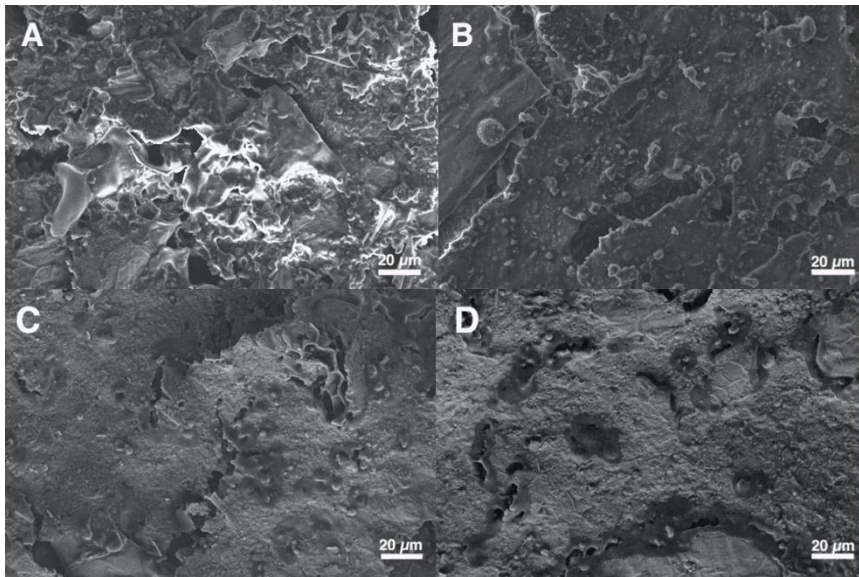


Figure 8

TABLE CAPTIONS

Table 1: Young's modulus, maximum tensile strength and Elongation at break of the different processed systems. Different letters within a column indicate significant differences ($p < 0.05$).

<i>System</i>	<i>E (MPa)</i>	σ_{\max} (MPa)	ε_{\max} (%)
<i>I50</i>	10 ± 1^A	0.12 ± 0.01^A	1.9 ± 0.2^{BC}
<i>I80</i>	33 ± 6^C	0.27 ± 0.01^B	2.4 ± 0.3^C
<i>I90</i>	20 ± 1^B	0.19 ± 0.01^C	2.5 ± 0.5^C
<i>I110</i>	10 ± 1^A	0.073 ± 0.006^D	1.4 ± 0.5^B
<i>I110*</i>	80 ± 1^D	0.43 ± 0.04^E	1.0 ± 0.1^A